COMMUNICATIONS: SIF Congress 2022

A didactic experiment to measure the angular correlation between the two gamma rays emitted by a ^{60}Co source(*)

R. Pirlo(^{1})(**) and N. Nicassio(^{1})(^{2})(***) on behalf of E. C. Amato(^{1}),
A. Anelli(^{1}), M. Barbieri(^{1}), D. Cataldi(^{1}), V. Cellamare(^{1}), D. Cerasole(^{1}),
F. Conserva(^{1}), S. De Gaetano(^{1})(^{2}), D. Depalo(^{1}), A. Digennaro(^{1}),
E. Fiorente(^{1}), F. Gargano(^{2}), D. Gatti(^{1}), P. Loizzo(^{1}), F. Loparco(^{1})(^{2}),
O. Mele(^{1}), G. Perfetto(^{1}), R. Pillera(^{1})(^{2}), E. Schygulla(^{1})
and D. Troiano(^{1})

(^{1}) *Dipartimento di Fisica M. Merlin, Università e Politecnico di Bari - Bari, Italy*
(^{2}) *Istituto Nazionale di Fisica Nucleare, Sezione di Bari - 70126, Bari, Italy*

Summary. — A didactic experiment carried out by a group of Physics masters' students at Bari University is presented. The purpose was the study of the angular correlation between the two gamma rays of 1.17 MeV and 1.33 MeV emitted in typical ^{60}Co decays by means of two NaI(Tl) scintillators equipped with photomultiplier tubes read out by a digital oscilloscope. Several runs were performed with the Co source at different angles between the two scintillators. Additional runs were performed removing the source, to study the backgrounds from cosmic rays and from gamma rays emitted by the radioactive isotopes ^{208}Tl and ^{40}K. Our results showed that the signal rate changes with the angular separation in agreement with the theoretical expectations by Hamilton dating back to 1940 and with recent measurements documented in the literature. Students learned to plan and set up an experiment, to take data and to perform basic analysis. Care was taken to understand the limits of our experimental apparatus and possible improvements.

1. – Introduction

Although NaI(Tl) scintillators were first introduced in the 1950s, they are still commonly used in X-ray and gamma-ray spectroscopy to detect photons with energies up to a few MeV [1] and are often available in educational laboratories for undergraduate physics students. Therefore, experiments with NaI(Tl) scintillators are highly recommended in laboratory courses on detectors.
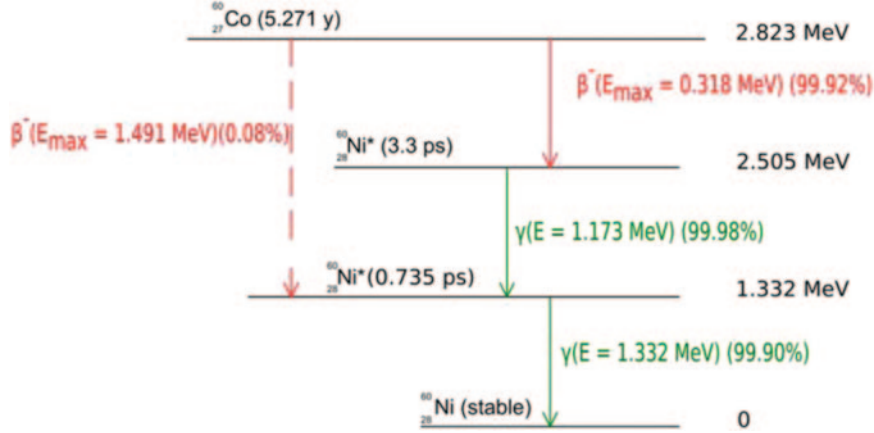

Fig. 1. – Diagram of the decay chain from ^{60}Co into ^{60}Ni.

We have designed and implemented a didactic experiment to measure the angular correlations between the two gamma rays emitted by a weak radioactive Cobalt-60 (^{60}Co) source using two NaI(Tl) scintillators readout with photomultiplier tubes (PMTs) already available in our laboratory, whose signals are processed by a digital oscilloscope. The experiment has been carried out by a class of undergraduate students, who attended the course of "Particle and Radiation Detector Laboratory" during the Master's Degree Course in Physics at the University of Bari.

The experiment described in this paper allowed the students to get to a better understanding of the interactions of photons with matter, to become familiar with scintillators and, above all, to be involved in all the stages of the experimental activity, setting up an experiment to validate a theoretical model on their own.

2. – Theoretical background

^{60}Co is a radioactive isotope of cobalt with a spin-parity $J^P = 5^+$ and with a half-life of 1925.20 ± 0.25 days [2, 3]. Its decay chain is shown in fig. 1. In particular, 99.88% of the times [4] it undergoes beta decay to an excited state of ^{60}Ni with a spin-parity $J^P = 4^+$, which subsequently decays, passing through the intermediate state $J^P = 2^+$, into the ground state $J^P = 0^+$ with the emission of two gamma rays, respectively with energies of 1.17 MeV and 1.33 MeV. Since the lifetime of the intermediate state is of the order of 10^{-12} s [5], much smaller than the typical experimental time resolutions, the two gamma rays are expected to be detected in coincidence.

From nuclear radiation theory it can be shown that the emission directions of consecutive gamma rays produced by an excited nucleus are correlated [6]. The angular correlation can be expressed in terms of the relative probability per unit solid angle $W(\theta)$ of the second photon to be emitted at an angle θ with respect to the first one. In particular, explicit quantum mechanical calculations by Hamilton show that, in the case of ^{60}Co, the angular correlation function is given by

$$(1) \qquad W(\theta) = 1 + \frac{1}{8}\cos^2\theta + \frac{1}{24}\cos^4\theta,$$
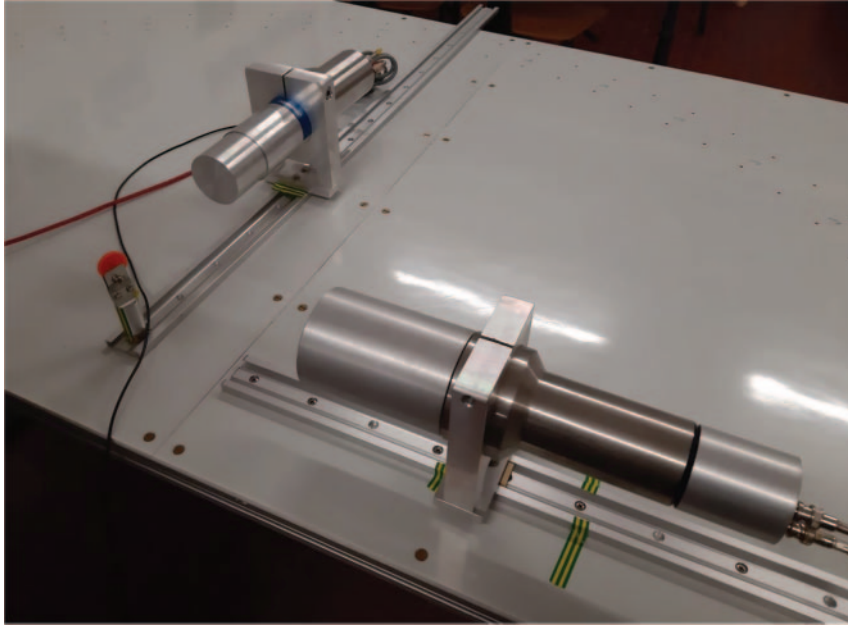
apart from a constant factor.

Fig. 2. – Photo of the experimental setup. The ^{60}Co source is placed in the holder at the center of the picture. The scintillators are mounted on rails pointing toward the source.

Different measurements of this correlation function were already performed in the past, and the results were in agreement with Hamilton's prediction (see for instance refs. [5, 7-10]). We implemented a didactic experiment to perform a measurement of $W(\theta)$ with a custom experimental setup in our laboratory [11].

3. – Experimental setup and trigger logic

A photo of the experimental setup is shown in fig. 2. A ^{60}Co disk-shaped source, 1 mm thick, with a diameter of 1 cm and an activity of ~ 5 kBq, was placed on a holder at the center of the setup. Two cylindrical NaI(Tl) scintillators coupled with PMTs, which could be moved along two rails, were used to detect the gamma rays from ^{60}Co decays. The first scintillator (S_0 hereafter), with a length of 8.2 cm and a diameter of 8.2 cm, was mounted on a fixed rail, while the second scintillator (S_1 hereafter), with a length of 5.8 cm and a diameter of 5.8 cm, was mounted on a mobile rail, which could be rotated around the source with respect to the fixed one. A graduated scale, divided in sections of 5° step between 0° and 180°, was drawn on the table to measure the angle between the two rails.

Measurements were performed by placing the scintillators S_0 and S_1, respectively at 20 cm and 14.1 cm from the source, so that the solid angle subtended by each scintillator with respect to the source was the same, amounting to $\Delta\Omega \simeq 0.132$ sr. The choice of the distances was driven by the need to keep a sufficiently high event rate during data taking while keeping a limited uncertainty on the angle between the scintillators. Indeed, the latter is determined by the radius of the two scintillators and by their distances from the source and it amounts to $\Delta\theta \sim 16°$. Adhesive tape was used to indicate the reference positions of the scintillators and of the holder for the source.
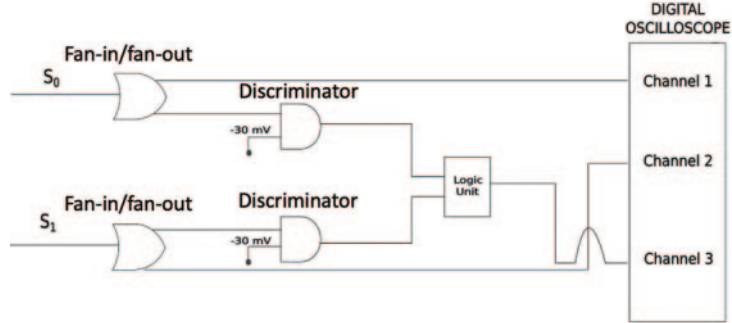
Fig. 3. – Schematic of the trigger logic.

The signals from the two PMTs were read out using a digital oscilloscope *Teledyne Le Croy WaveRunner 6 Zi* [12]. The trigger logic used for data acquisition is shown in fig. 3. The analog signals from the PMTs coupled with S_0 and S_1 were sent to two linear fan-in/fan-out modules, producing two copies of each input signal. A copy of the two signals from S_0 and S_1 was sent directly to the oscilloscope (Channel 1 and Channel 2 in the scheme of fig. 3). The second copy was sent to a discriminator module with a threshold set at -30 mV. The logic output signals from the discriminator were then sent to a logic unit, where the trigger to the oscilloscope was formed (channel 3 in the scheme of fig. 3).

Our measurements were performed using the following trigger configurations:

- "and" configuration: signals from both S_0 and S_1 were required in order to select events with a γ-ray in both scintillators.

- "or" configuration: a signal from either S_0 or S_1 was required in order to perform energy calibrations.

An example of the analog signals from the two scintillators in the "and" trigger configuration can be seen in fig. 4. As expected, the signals exhibit a rise time of about 15 ns, determined by the RC constant of the readout circuit, and a fall time of about 230 ns, determined by the decay time of the fluorescence light in the NaI scintillators.
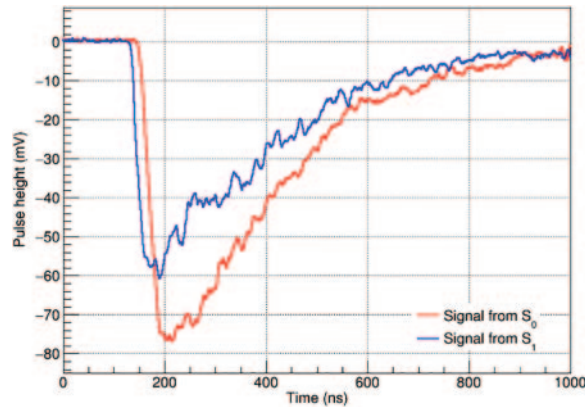

Fig. 4. – Example of the analog signals produced in the two scintillators by the gamma rays emitted from the ^{60}Co source.
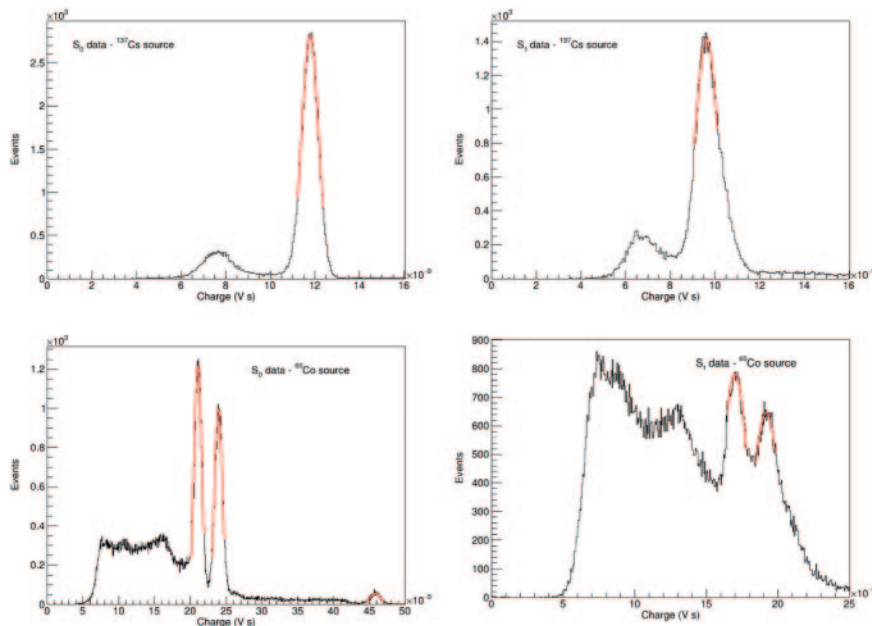
Fig. 5. – Charge distributions obtained with the ^{137}Cs source (top row) and with the ^{60}Co source (bottom row). The plots on the left column refer to the scintillator S_0, while those on the right column refer to the scintillator S_1.

The oscilloscope was then used to measure the charge of the pulses from the PMTs, and data were stored in ROOT files [13] for later analysis.

4. – Energy calibration

The starting point for our analysis was the energy calibration, needed to convert the charge of the signals read out by the oscilloscope into the corresponding energy depositions in the scintillators. For the calibration we used the ^{60}Co source, providing calibration points at $1.17\,\mathrm{MeV}$ and $1.33\,\mathrm{MeV}$, and a ^{137}Cs source, providing a calibration point at $0.662\,\mathrm{MeV}$ [4]. Moreover, an additional point, corresponding to the sum of the energies of the two photons from the ^{60}Co source ($2.50\,\mathrm{MeV}$), was included in the calibration of S_0, since both gamma rays could be absorbed in the same scintillator. This point was not available for the calibration of S_1 because, due to its reduced size, the probability of both photons being absorbed in S_1 was negligible and its energy resolution was poor. Finally, a further calibration point was provided by the pedestal peak, corresponding to a null energy deposition in the scintillators. The position of the pedestal peak in each scintillator was evaluated from its charge distribution in a run with the ^{137}Cs source, triggering the other scintillator.

The measured charge distributions for the calibration runs performed with the ^{60}Co and ^{137}Cs sources are shown in fig. 5. The full-energy peaks were fitted with Gaussian functions to get the corresponding charges. From the linear fit of the calibration points we got the calibration curve shown in fig. 6. The fits to the charge distributions were also used to compute the energy resolution σ_E/E. For the ^{60}Co photon energies, in the MeV region, we found a resolution of about 2.5% for S_0 and of about 5.0% for S_1.
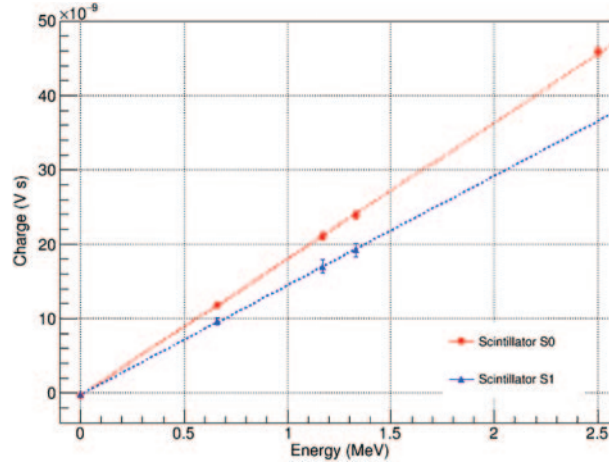
Fig. 6. – Energy calibration curves for the two scintillators.

5. – Data analysis

To measure the angular correlations between the gamma rays emitted in the ^{60}Co decays, we performed several runs in the "and" trigger configuration changing the angle between the two detectors. For each angle, runs both with and without the ^{60}Co source were performed, the latter being required to evaluate the background rates due to natural radioactivity and cosmic rays penetrating in our laboratory.

Figure 7 shows the average rate of events as a function of the energies E_0 and E_1 deposited in the two detectors. The following regions can be identified in the plot:

- The two peaks at the positions $(1.17\,\text{MeV}, 1.33\,\text{MeV})$ and $(1.33\,\text{MeV}, 1.17\,\text{MeV})$ correspond to events with full energy deposition of both ^{60}Co gamma rays in the two scintillators. Each photon has likely undergone a photoelectric interaction with the scintillator material, and the resulting photoelectron has been absorbed in the scintillator.

- The vertical and horizontal bands adjacent to the peaks correspond to events where the photon absorbed in one of the two scintillators releases its whole energy, while the photon absorbed in the other scintillator releases only a fraction of its energy. In this case, the second photon has likely undergone a Compton scattering, with the electron being absorbed in the scintillator and the scattered photon escaping from the detector. The lower event rate observed for the horizontal bands is due to the smaller size of S_1 with respect to S_0.

- The diagonal bands centered on the lines $E_0 + E_1 = 1.17\,\text{MeV}$ and $E_0 + E_1 = 1.33\,\text{MeV}$ correspond to events where one of the two photons undergoes Compton scattering in a scintillator, with the scattered photon being absorbed by the other scintillator.

- The diagonal band centered on the line $E_0 + E_1 = 2.50\,\text{MeV}$ corresponds to events where the first photon is absorbed in one of the two scintillators, while the second photon undergoes Compton scattering in the same scintillator and the scattered photon is absorbed in the other scintillator.
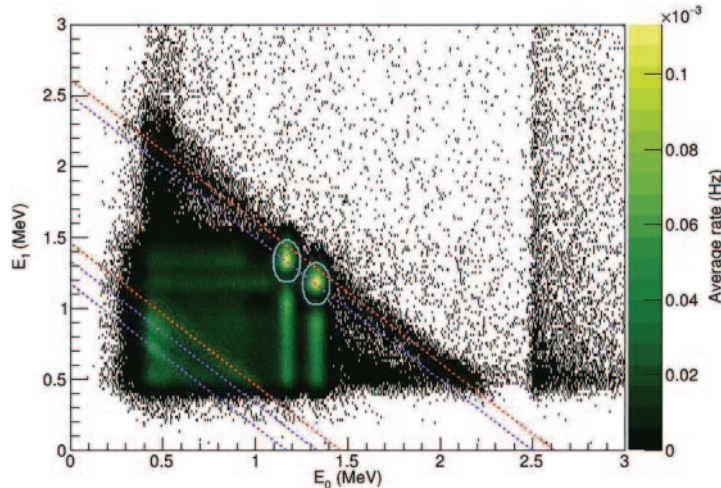
Fig. 7. – Average rate of events as a function of the energy deposited in the two scintillators in the runs with the ^{60}Co source. The dashed lines correspond to the energies of the two photons emitted by the ^{60}Co source (1.17 MeV and 1.33 MeV), to the sum of the energies of both photons (2.50 MeV) and to the energies of photons produced in the decays of ^{40}K (1.461 MeV) and ^{208}Tl (2.610 MeV). The continuous lines indicate the ellipses used for the event selection.

- The diagonal bands centered on the lines $E_0 + E_1 = 1.46$ MeV and $E_0 + E_1 = 2.61$ MeV correspond to background events where a gamma ray from the decays of ^{40}K or ^{208}Tl undergoes Compton scattering in a scintillator with the scattered photon being absorbed in the other scintillator. These decays mostly originate from the ^{40}K in the glass windows of the PMTs and from the ^{208}Tl in the scintillators.

- The region $E_0 > 2.5$ MeV which is populated by events where both photons from the ^{60}Co decays or the gamma ray from the ^{208}Tl decay are fully absorbed in S_0, in coincidence with a cosmic-ray event in S_1.

The distribution of the energy depositions in the two scintillators in the runs without the ^{60}Co source are then shown in fig. 8. From the comparison with fig. 7, a significant rate drop is observed in the regions corresponding to ^{60}Co gamma rays, while the diagonal bands corresponding to gamma rays from ^{40}K and ^{208}Tl decays become more evident. Additional and less populated diagonal bands corresponding to photons produced in the decays of other radioactive isotopes are also visible.

To suppress the contribution due to background events, in our analysis we selected events in the regions corresponding to the two peaks shown in fig. 7. The selection was performed discarding events outside the ellipses defined by the following equations:

$$\text{(2)} \qquad \frac{(E_0 - 1.33\,\text{MeV})^2}{a^2} + \frac{(E_1 - 1.17\,\text{MeV})^2}{b^2} = 1,$$

$$\text{(3)} \qquad \frac{(E_0 - 1.17\,\text{MeV})^2}{a^2} + \frac{(E_1 - 1.33\,\text{MeV})^2}{b^2} = 1,$$

where $a = 0.075$ MeV and $b = 0.150$ MeV. The values of a and b were set to about 3 times the energy resolutions of S_0 and S_1 at 1 MeV. The contours of the ellipses in eqs. (2) and (3) are shown in the plots of figs. 7 and 8.
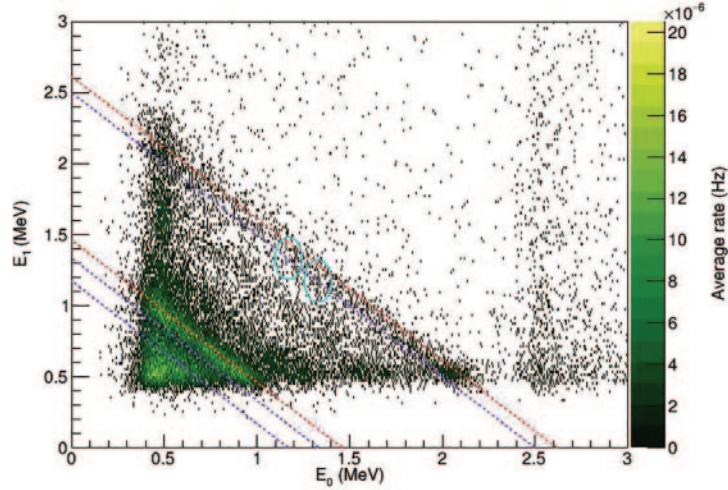
Fig. 8. – Average rate of events as a function of the energy deposited in the two scintillators in the runs without the ^{60}Co source. The lines have the same meanings as in fig. 7.

6. – Results and conclusions

We performed several measurements, changing the opening angle between the two scintillators in the range between 90° and 180° with 15° steps. The event selection illustrated in sect. **5** was applied to the runs taken in the different configurations explored. The signal rate at each angle was evaluated as the difference between the rate of selected events with and without the ^{60}Co source. Our results are summarized in fig. 9.

To check the compatibility with the theoretical prediction, the experimental data have been fitted with the function

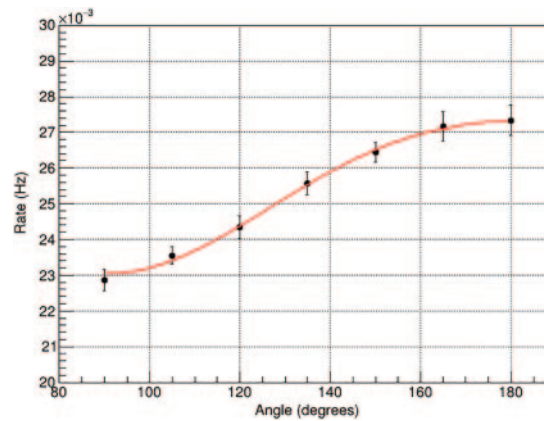$$(4) \qquad\qquad r(\theta) = r_0 \left(1 + a \cos^2 \theta + b \cos^4 \theta \right),$$

Fig. 9. – Average rate of signal events as a function of the opening angle between S_0 and S_1. The red line represents the fit function.

where r_0 corresponds to the rate when the angle between the two scintillators is $90°$ and the expected values of the parameters a and b, according to Hamilton's theoretical model, are 0.125 and 0.042, respectively. In our fit we find the values $r_0 = (2.303 \pm 0.021) \times 10^{-2}$ Hz, $a = 0.249 \pm 0.058$ and $b = (-6.43 \pm 5.88) \times 10^{-2}$ with a $\chi^2/d.o.f. = 0.77/4$.

As expected, the signal rate increases when increasing the opening angle between the two scintillators. However, we find a discrepancy of about two sigma on both the correlation coefficients a and b with respect to theoretical predictions. These discrepancies can be due to several reasons. A possible cause could be the finite size of the ^{60}Co source used in our measurement. Hamilton's model assumed a pointlike radioactive source. However, as discussed in sect. **3**, our source was encapsulated in a disk having a thickness of $1\,$mm and a diameter of $1\,$cm. When the mobile scintillator was rotated (see fig. 2) the projected cross section of the source on the front area of the mobile scintillator changed with the rotation angle. In addition, in our setup we used a low-activity source and we had to place the scintillators very close to the source to keep a sufficiently high event rate during data taking. As discussed in sect. **3**, this configuration implies an uncertainty on the opening angle which, on the basis only of pure geometrical considerations, is of about $16°$. Placing the scintillators at larger distances from the source would allow the minimization of this uncertainty.

Some precautions could be taken to improve our results. First of all, two larger scintillators (*i.e.*, at least with the size of S_0 in our setup) could enhance the probability that both gamma rays deposit their whole energy within the detector volumes. Then, a source with a higher activity would be an upgrade, allowing the scintillators to be placed at larger distances, thus improving the precision in the angle definition. Finally, the effects of possible asymmetries in the shape of the source could be minimized using a rotating source.

REFERENCES

[1] KNOLL GLENN F., *Radiation Detection and Measurement* (John Wiley & Sons) 2010.
[2] UNTERWEGER M. P., HOPPES D. D. and SCHIMA F. J., *Nucl. Instrum. Methods Phys. Res. A*, **312** (1992) 349.
[3] UNTERWEGER M. P., *Appl. Radiat. Isotopes*, **56** (2002) 125; *Conference on Radionuclide Metrology and Its Application (ICRM 2001), May 14-18, 2001*.
[4] Data taken from the Laboratoire National Henri Bequerel online database, `http://www.lnhb.fr/nuclear-data/module-lara/` (accessed: 2021-12-01).
[5] BRADY E. L. and DEUTSCH M., *Phys. Rev.*, **78** (1950) 558.
[6] HAMILTON D. R., *Phys. Rev.*, **58** (1940) 122.
[7] GOOD WILFRED M., *Phys. Rev.*, **70** (1946) 978.
[8] COLOMBO S. R. A. and SCOTTI A., *Il Nuovo Cimento*, **2** (1955) 471.
[9] SMITH J. K., MACLEAN A. D., ASHFIELD W., CHESTER A., GARNSWORTHY A. B. and SVENSSON C. E., *Nucl. Instrum. Methods A*, **922** (2019) 47.
[10] KLEMA E. D. and McGOWAN F. K., *Phys. Rev.*, **91** (1953) 616.
[11] AMATO E. C. *et al.*, *Eur. J. Phys.*, **43** (2022) 055802.
[12] WaveRunner 6 Zi and HRO Operator's Manual, `https://cdn.teledynelecroy.com/files/manuals/waverunner-6zi-operators-manual.pdf`, accessed: 2021-10-01.
[13] BRUN R. and RADEMAKERS F., *Nucl. Instrum. Methods A*, **389** (1997) 81.